



Projected changes in the heatwave's characteristics and associated population exposure over India under 1.5–3 °C warming levels

Hardeep Kumar Maurya¹ · Nitin Joshi¹ · Shakti Suryavanshi²

Accepted: 22 February 2024 / Published online: 18 March 2024

© The Author(s), under exclusive licence to Springer-Verlag GmbH Germany, part of Springer Nature 2024

Abstract

In this study changes in the heatwave characteristics and associated population exposure for the five months (March–July) of the year is examined over India. The study considered 1.5 °C, 2 °C, and 3 °C global warming levels (GWL) and for two time periods, i.e., the near future (T1; 2021–2050) and the distant future (T2; 2071–2100) using the Coupled Model Inter-comparison Phase 6 (CMIP6) framework. This study identifies the heatwave using the extreme heatwave factor (EHF). The findings demonstrate a significant rise in mean summer heatwave frequency, duration, and severity with increasing GWLs. With the increase in GWLs, most of the regions of India would face severe heatwave but the Himalayan, Coastal, and North-east regions are the most vulnerable to heat waves and associated severity. The March (18-fold) and April (9-fold) months show the maximum increase in severity compared to the months of May, June, and July from the current world (1991–2020). The population exposure showed significant regional variations, with the Coastal and Northeast regions seeing the highest exposure for all SSPs and warming periods, and the Himalayan region experiencing the lowest exposure. Comparing the population under all SSP, climate change contributes more to total exposure. The total exposure increases 1.4–1.6 folds from 1.5 to 2 °C GWL under all SSPs over India.

Keywords CMIP6 · Global warming · EHF · Heatwave severity · Population exposure

1 Introduction

The earth's temperature has already reached 1.2 °C above pre-industrial levels (WMO 2020; IPCC 2021). If the current rate of warming persists, it is projected that earth's temperature will reach 1.5 °C above pre-industrial levels by 2030–2040. Climate models predict that the global temperature will rise in the future and may reach 5.5 °C by the end of the century (Mazdiyasi et al. 2017; IPCC 2014). This increasing global temperature is expected to lead to a substantial increase in the frequency, duration, and intensity

of extreme weather events, such as extreme precipitation, droughts, heat waves, etc. (Li et al. 2020). Heat waves are a major environmental hazard that affects millions of people worldwide, causing adverse health effects (such as dehydration, heat stroke, heat exhaustion, etc.), crop losses, increased energy demand, increased evapotranspiration, intensification of drought, and economic damages (Mazdiyasi et al. 2017; Nishant et al. 2022; IPCC 2014). Urban areas tend to be significantly warmer than rural areas due to the urban heat island effect (Nishant et al. 2022; IPCC 2014) which poses additional risks to vulnerable high-density populations during heat waves, especially in the summer season.

Recent studies have exhibited that exposure to heat waves has increased globally (Zhou et al. 2022), particularly in low-income countries where populations are vulnerable to extreme heat. The highest increases in heatwave exposure was observed in Asia and Africa (Li et al. 2020). Heatwaves caused approximately 166,000 deaths worldwide between 1998 and 2017 (Rohini et al. 2019; Jyoteeshkumar Reddy et al. 2021). Zhou et al., (2022) found a significant increase in heatwave mean and peak intensity across West USA, Brazil, South Africa, West Asia, Central Asia, and Australia

✉ Nitin Joshi
nitin.joshi@iitjammu.ac.in

Hardeep Kumar Maurya
2018rce0039@iitjammu.ac.in

Shakti Suryavanshi
suryavanshi.shakti@gmail.com

¹ Department of Civil Engineering, Indian Institute of Technology Jammu, Jammu and Kashmir, India

² National Institute of Hydrology, Roorkee, India

whereas, an increase in heatwave frequency and duration over the US, Eurasia, and North Africa in the future period (2070–2100). The previous studies investigated the population exposure to extreme temperatures across the globe and revealed significant increases in Southeast Asia, South Asia, Africa, the United States (US), and North America (Smirnov et al. 2016; Liu et al. 2017; Andrews et al. 2018; Harrington and Otto 2018; Zhang et al. 2018; Rohat et al. 2019). Andrews et al., (2018) reported that as the warming increased to 3 °C from the pre-industrial era, the risk of extreme heat stress would affect a much larger area and the number of high-risk heat-exposed countries would double (with more than 10 million people).

India is vulnerable to heat waves due to its high population density, limited access to air conditioning, and rapidly changing climate. Extreme temperature events combined with high population growth could have a significant impact on Indian society in terms of severe heat stress and increased mortality (McMichael et al. 2008). In India, heat waves occur between March–June and cause severe human health impacts (Pai et al. 2013; Pattanaik et al. 2017; Rao et al. 2023). The severity of heat mortality caused 27,366 deaths across India between 1992 to 2019. Most of the casualties happened in the eastern coastal region of India during the summer period (Guleria 2018; Rohini et al. 2019; Nageswararao et al. 2020). Several studies have documented an increasing trend in heat waves and their severity in India in recent years and near-future (Rohini et al. 2016; Mishra et al. 2017; Mukherjee and Mishra 2018; Singh et al. 2021; Rao et al. 2023). Rohini et al. (2019) report an increase in heatwave events and their duration 2020 to 2064 period. Heatwave trends were particularly pronounced over the north-western and south-eastern coastal regions of India (Ratnam et al. 2016; Rohini et al. 2016). Rao et al. (2023) studied heatwave characteristics for the near and far future over India and found a significant increase in frequency, magnitude duration, and season length of summertime heatwaves. Mishra et al. (2017) reported that population exposure to severe heatwaves is expected to increase by 15 and 92 times from the current level (1986–2015) by the middle and end of the century, respectively over India. Das et al. (2022) analysed population exposure to compound extreme events in India for two future periods and found that Central Northeast India would have the highest total exposure whereas, hilly terrain would exhibit the lowest exposure. The previous studies also highlighted the need for effective heat wave management strategies (Mishra et al. 2017; Mukherjee and Mishra 2018).

It is therefore crucial to study heat wave characteristics and associate population exposure at a regional level in the context of global warming levels. However, no single approach or set of criteria can monitor or classify heat waves worldwide or regionally (Perkins and Alexander 2013). The

warming of the surface temperature is non-uniform with different degrees of tolerance (Nageswararao et al. 2020). Keeping in view, heat wave indices defined by temperature threshold (intensity) and number of consecutive days of exceeding the threshold (duration) were utilised to understand the impact of the heatwave and associated mortality (Andrews et al. 2018; Mukherjee and Mishra 2018; Oleson et al. 2018; Dahl et al. 2019; Nori-Sarma et al. 2019). For the current study, we used the Excess Heat Factor (EHF) to define the heat wave. The severity of the EHF has been widely used for assessing exposure and its correlation with human health impact across the globe (Nairn et al. 2018).

According to the reports released by the Intergovernmental Panel on Climate Change (IPCC) and the 26th United Nations Climate Change Conference of the Parties (COP26), the primary objective is to mitigate global warming to a maximum increase of 1.5 °C (Dwivedi et al. 2022; COP26 2021). While earlier studies (Rohini et al. 2016, 2019; Mishra et al. 2017; Rao et al. 2023) have predominantly concentrated on prospective temporal periods (historical, near future, and far future), our investigation redirects its focus toward the examination of distinct degrees of warming, specifically 1.5 °C, 2 °C, and 3 °C above pre-industrial level. There exists a dearth of studies that have examined alterations in heatwave characteristics and the corresponding exposure of populations across various levels of warming. Heatwave events exhibit significant regional variability. The utilisation of this focused methodology enables us to investigate the distinct attributes of heatwaves within temperature-homogenous areas of India at critical thresholds and better aligns with the Paris Agreement's objectives.

The following research questions are addressed in the present study (1) How well different climate models can capture the summer mean temperature pattern and heatwave characteristics (heatwave severity frequency, duration, intensity, etc.) over India. (2) How would the heatwave characteristics and associated population exposure change under 1.5 °C, 2 °C, and 3 °C global warming scenarios compared to the base period (1971–2000)? (3) How much the population growth and climate change contribute to the total exposure?

2 Study area and datasets

Figure 1 shows seven homogeneous temperature regions classified by the Indian Institute of Tropical Meteorology (IITM) based on topographical, geographical, and climatological features namely the east coast (EC), interior peninsula (IP), north central (NC), northeast (NE), northwest (NW), western Himalaya (WH), and west coast (WC). This classification has been widely used to study the changes in temperature in India (Kothawale and Rupa Kumar 2005;

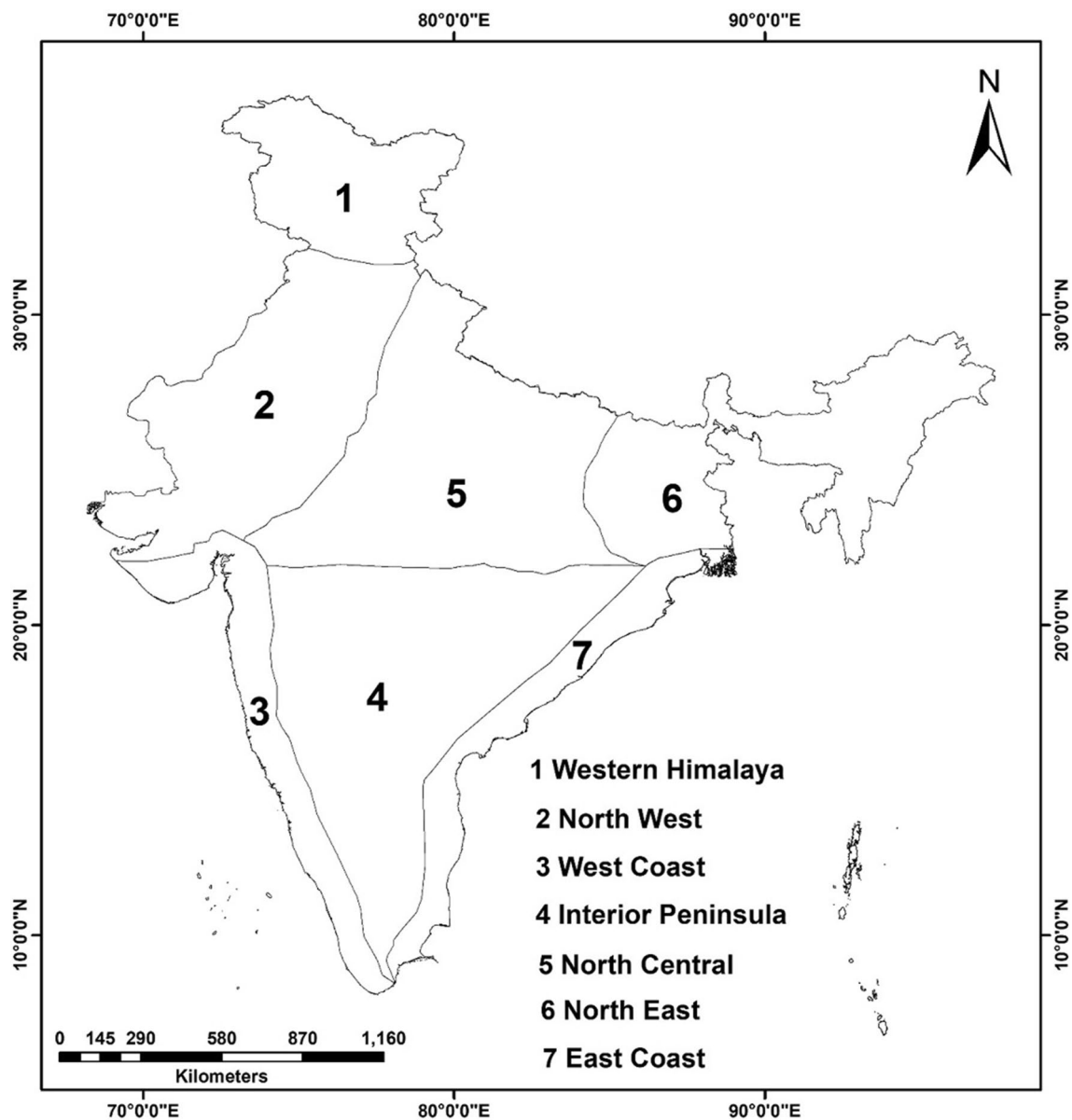


Fig. 1 Study area showing homogeneous temperature regions of India

Dash and Mamgain 2011; Sonali and Kumar 2013; Maurya et al. 2023).

The study uses observed gridded daily maximum and minimum temperature datasets from the National Climatic Centre (NCC), Indian Meteorological Department (IMD) for 1951–2014, which have been developed using a modified Shepard's angular distance weighting interpolation algorithm. The datasets have a resolution of $1^\circ \times 1^\circ$ and cover a spatial domain of 7.5° N to 37.5° N and 67.5° E to 97.5° E, with a few grids excluded from the analysis. The study uses 13 bias-corrected CMIP6 climate models to estimate the changes in heatwave characteristics for the future period, with the minimum and maximum temperature datasets at

0.25° resolution developed by Mishra et al. (2020). All the data sets used in the study were further re-gridded at $0.5^\circ \times 0.5^\circ$ resolution using a linear interpolation technique. For the analysis, a base period of 1971–2000 was assumed.

The Shared Socioeconomic Pathways (SSPs) are scenarios that define future greenhouse gas emissions based on assumptions regarding economic and population growth, investments in health and education, land use, air pollution, energy systems, and climate mitigation efforts. In this study, we focused on four SSP scenarios, namely SSP1-2.6, SSP2-4.5, SSP3-7.0, and SSP5-8.5. To assess population exposure to heat wave events, we used gridded population datasets at $1/8^\circ$ resolution for SSP1, SSP2, SSP3, and SSP5. The

population datasets were obtained from the Socioeconomic Data and Applications Centre (SEDAC) from 2000 to 2100 and re-gridded at 0.5-degree spatial resolution. The datasets are available at a 10-year interval and were linearly interpolated to an annual time step. The global population data are categorized into different pathways, including SSP1 (sustainability) and SSP5 (fossil fuel development), which both assume low population growth in high-fertility countries and high urbanization in most regions of the globe, but differ in economic growth. SSP1 assumes medium economic growth, while SSP5 assumes high economic growth. SSP2 (middle of the road) is considered to have medium growth in population, urbanization, and economic growth, while SSP3 (regional rivalry) assumes high population growth and low urbanization, with low economic growth.

3 Methodology

The warming periods are the time intervals in which the global mean temperature increases to a certain level of warming (such as 1.5, 2.0, and 3.0 °C) above the pre-industrial era (1881–1910). We used the time-slice method to calculate the warming periods (Schleussner et al. 2016; Li et al. 2018; Yu et al. 2018; Singh and Kumar 2019). The details of the models and their warming are presented in Table S1. We calculated the heatwave characteristics and associated population exposure for 1.5, 2.0, and 3.0 °C GWL and for the near future (T1, 2021–2050) and the far future (T2, 2071–2100). Since the mean temperature for the summer season is used to define the heatwaves therefore, we calculate the model's bias for the March, April, May, June, and July months. Generally, a heatwave is a period where temperatures consistently exceed a predefined threshold (which may be fixed or based on a percentile) (Raei et al. 2018). Here, we use the method developed by Nairn and Fawcett, (2011) based on three-day-averaged daily mean temperature to identify the heatwave intensity, duration, and its severity for five months (March–July) of the year.

3.1 Excess heat factor (EHF)

EHF is a metric that is used to measure the severity of extreme heat events. The EHF index is a combination of the maximum temperature, the duration of the heat event, and the rate of temperature change. EHF considers the impact of nocturnal temperatures and provides an overall measure of the intensity and duration of an extreme heat event and can be used to compare heat events across different regions and periods. Also, it provides spatial distribution by accounting for local geographic acclimatization, heat load, and recent temperature variation (Nairn and Fawcett 2014; Keggenhoff et al. 2015).

EHF was introduced by Nairn and Fawcett, (2011) and widely used in previous studies (Keggenhoff et al. 2015; Raei et al. 2018; Zhou et al. 2022; Rao et al. 2023; Reddy et al. 2021; Nairn et al. 2018). EHF is the combined effects of two indices, excess heat (EHI_{sig}) and heat stress (EHI_{accl}). These indices are defined as:

$$EHI_{sig} = \left(\frac{T_i + T_{i+1} + T_{i+2}}{3} \right) - T_{95} \quad (1)$$

where EHI_{sig} is significance of heat event and T_i is the daily mean temperature at day i and T_{95} is the 95th percentile of daily mean temperature of the base period (1971–2000). Recent past heat stress quantifies heat event (EHI_{accl}) is define as,

$$EHI_{accl} = \left(\frac{T_i + T_{i+1} + T_{i+2}}{3} \right) - \left(\frac{T_{i-1} + T_{i-2} + \dots + T_{i-30}}{30} \right) \quad (2)$$

where $\left(\frac{T_{i-1} + T_{i-2} + \dots + T_{i-30}}{30} \right)$ is the recent past 30 days mean temperature from day i . EHF is the combined effect of EHI_{sig} and EHI_{accl} .

$$EHF = \max(0, EHI_{sig}) \times \max(1, EHI_{accl}) \quad (3)$$

We considered EHF (°C²) is positive as thresholds for heatwave. Heatwave is considered if three consecutive days are greater than 0.

$$EHF_{Severity} = \frac{EHF}{EHF_{85}} \quad (4)$$

EHF_{85} is 85th percentile of all positive EHF for the base period. To agree with the annual temporal resolution of daily $EHF_{Severity}$ values were summarised into annual maximum severity time series.

3.2 Heatwave indices

EHF is used to identify the heatwave days in the present study. Positive value of EHI_{sig} define heatwave like conditions for i th day. If $\left(\frac{T_i + T_{i+1} + T_{i+2}}{3} \right) > T_{95}$ for at least three consecutive days, then these days are considered as heatwave. Once the heatwave days are defined, different characteristics of heatwave can be calculated. All the calculated heatwave characteristics indices based on duration (HWD, HWAS, and HWSL), frequency (HWN and HWF) and intensity (HWMI and HWAI) are defined in Table 1.

To assess the spatial agreement between a reference and each Regional Climate Model (RCM), we employ the Spatial Efficiency (SPAEF) and Percent Bias (PBIAS) (Koch et al. 2018; Petrovic et al. 2023). SPAEF is a comprehensive performance measure that evaluates the similarity of spatial patterns. It is defined as:

Table 1 Details of heatwave indices calculated based on the Excess Heat Factor (EHF)

Abbreviations	Indices	Definition	Unit
HWN	Annual heat wave number	Total number of the annual summer (March–July) heat waves events where conditions persist for at least 3 consecutive days with positive EHF values	Number of events
HWF	Annual heatwave frequency	Number of Heatwave days relative to the total number of days (March–July)	%
HWD	Longest heat wave duration	The length of the longest summer (March–July) heat wave	Days
HWAS	Annual average heatwave Spell	The average length of all summer (March–July) heat wave spells	Days
HWMI	The annual maximum intensity of heatwave	Maximum magnitude of all summer (March–July) heat wave days	°C
HWAI	The annual average intensity of heatwave	Average magnitude of all summer (March–July) heat wave days	°C
HWSL	Duration of the annual heatwave	Total length of the summer (March–July) heat wave where conditions persist for at least 3 consecutive days with positive EHF values	Days

$$SPAEF = 1 - \sqrt{(\alpha - 1)^2 + (\beta - 1)^2 + (\gamma - 1)^2} \tag{5}$$

where α is the Pearson correlation coefficient between observed and simulated patterns, β is the fraction of the coefficient of variation representing spatial variability and calculated as:

$$\beta = \left(\frac{\sigma_{sim}}{\mu_{sim}} \right) / \left(\frac{\sigma_{obs}}{\mu_{obs}} \right) \tag{6}$$

And γ is the minimum of the overlapped histograms of the observed (K) and simulated (L) patterns with the same number of bins (n) expressed as:

$$\gamma = \frac{\sum_{i=1}^n \min(K_i, L_i)}{\sum_{i=1}^n K_i} \tag{7}$$

To calculate γ , the z score of the patterns is utilized, enabling the comparison of variables with different units. The count of values in each bin i is determined for both K and L histograms. Then, the minimum count between K_i and L_i is selected for each bin, indicating the number of shared values in that bin. These numbers are subsequently summed and divided by the total number of values (n) in either K or L . The SPAEF is a metric that ranges from $-\infty$ to 1, where 1 represents perfect agreement between the two patterns. The three components of SPAEF are independent of each other and typically carry equal weightage, complementing each other to provide comprehensive pattern information. Instead of focusing on precise grid-scale values, this approach evaluates global features such as distribution and variability, offering holistic assessment of the patterns (Koch et al. 2018).

To assess the accuracy and reliability of climate models we calculate PBIAS. It provides an indication of the

overall bias or systematic deviation of the model's results from the observed data.

$$PBIAS = 100 * \left[\frac{\sum_{i=1}^n (\bar{Q})}{\sum_{i=1}^n \bar{O}} - 1 \right] \tag{8}$$

\bar{Q} is the mean of simulation, \bar{O} is the mean of observed. An ideal PBIAS value is 0, indicating a model that accurately simulates the observed data. PBIAS values with a small magnitude suggest a good match between simulated and observed values. Positive PBIAS values indicate a bias of overestimation in the model, while negative values indicate a bias of underestimation.

3.3 Population exposure

The population's exposure to heatwave can be determined by multiplying the number of heatwave days with the population affected. To identify heatwave days, a threshold of the 95th percentile of daily maximum temperature with three consecutive days was used, which was calculated for each grid based on base period. The method proposed by Jones et al. (2015) was used to calculate the total change in exposure, which has been used in various studies. Additionally, the study examined the impact of both population growth and climate change on total exposure. Other studies (Liu et al. 2017; Chen and Sun 2019, 2021; Chen et al. 2020; Weber et al. 2020; Das et al. 2022) have also used this approach. The contribution of population and climate change on total exposure was calculated by Eq. (9).

$$\Delta E = P_1 \times \Delta C + C_1 \times \Delta P + \Delta C \times \Delta P \tag{9}$$

ΔE is the total change in exposure, ΔC and ΔP are the change in HWD and population from the base period

(1971–2000) to 1.5, 2, and 3 GWL. $P_1 \times \Delta C$, $C_1 \times \Delta P$, and $\Delta C \times \Delta P$ are the population, climate and their interaction effect. The contribution rate of each factor was calculated by:

$$C = \frac{\Delta C \times P_1}{\Delta E} \times 100 \quad (10)$$

$$P = \frac{\Delta P \times C_1}{\Delta E} \times 100 \quad (11)$$

$$I = \frac{\Delta C \times \Delta P}{\Delta E} \times 100 \quad (12)$$

where C , P , and I represent the percentage changes in the climate, population, and interaction of population and climate respectively.

4 Results

4.1 Performance evaluation of historic climate simulations

The performance of Global Climate Models (GCMs) and Regional Climate Models (RCMs) in simulating observed data can be assessed using various quantifiable measures. In this study, three indicators were used to evaluate the performance of 13 historic CMIP6 temperature datasets from 1951 to 2014, compared to the gridded IMD temperature datasets observed during the same period. The three indicators used for evaluation were the mean of the temperature, PBIAS, and SPAEF. The performance of the models was analyzed and presented in Table 2. Most models underestimated the mean temperature and exhibit the bias ranging between -0.05% to -0.03%, except for NorESM2-MM, which showed an overestimation by 24.15%. On the other hand, all models demonstrated good spatial agreement with the observed data, with SPAEF values ranging from 0.33 to 0.36. The mean temperature of each of the models shows relatively close to the observed mean temperature except for NorESM2-MM. Based on the performance of models, 12 best-performing models were selected for further ensemble analysis. The ensemble of these 12 models showed acceptable spatial agreement (SPAEF of 0.31) and a small underestimation bias (PBIAS of -0.04%). These findings indicate that the selected ensemble of models performed well in replicating the observed temperature data, suggesting their suitability for further analysis for climate modeling studies.

We calculated the PBIAS and SPAEF for the indices (Table 2). All selected 12 models show an overestimation of bias for all the indices except for HWMI. However, the ACCESS-ESM1-5 model exhibited an underestimation of

bias, with a negative bias of -0.15% for HWN. The highest bias for the HWN was observed in the MRI-ESM2-0 model. However, For the HWAS, HWD, and HWAI indices, all models consistently overestimated the bias. The ranges for overestimation were 7% to 58% for HWAS, 8% to 58% for HWD, and 0.7% to 1.5% for HWAI. Among the models, MPI-ESM1-2-LR shows the highest PBIAS for these indices. Whereas, all the models show an underestimation of bias (range from -20 to -3.5%) for HWMI. The SPAEF values, which assess the spatial pattern and structure reproduction, are negative or very low for all models compared to the reference data. This indicates a lack of satisfactory reproduction of the spatial characteristics across all calculated indices. The higher SPAEF score is found for EC-Earth3-Veg, while MPI-ESM1-2-LR shows the lowest SPAEF value for all the indices. To summarize the model performance based on SPAEF and PBAIS, the ACCESS-ESM1-5 model demonstrated the best performance for the HWN index, while the MPI-ESM1-2-LR model exhibited the weakest performance. For the HWAS and HWD indices, the BCC-CSM2-MR model showed the best performance, while the MPI-ESM1-2-LR model displayed the weakest performance. Regarding the HWAI index, the ACCESS-CM2 model performed the best, while the BCC-CSM2-MR model showed the weakest performance. Whereas, MRI-ESM2-0 model achieved the best performance for the HWMI index, while the MPI-ESM1-2-LR model displayed the weakest performance.

4.2 Changes in extremes HW indices

We analysed the characteristics of heatwaves and their severity in different global warming scenarios. Figure 2 shows the ratio of all India averaged heatwave indices for 2001–2086 period with respect to the base period. Figures 3 and 4 show the ratio of the spatial distribution of all heatwave indices. Figures S1 and S2 show the change in spatial distribution and Fig. S3 and S4 show the change in the regional mean for heatwave indices (HWN, HWD, HWAS, HWF, HWMI, and HWAI) under 1.5 °C, 2 °C, and 3 °C scenario and period T1 and T2. All scenarios project an increase in heatwave indices in the future, the high emission scenarios SSP5-8.5 display the highest increment at the end of the century, while SSP1-2.6 shows the lowest (Figs. S7–S10). For all three three-warming scenarios HWN increases over most of the regions of India except at a few grid points in the WH, WC, and NE regions. The all India mean HWN increased by 2.2, 2.8, and 4-folds (14.82, 24, and 41.42 events) under 1.5, 2, and 3 °C GWL, respectively compared to the base period with more than 70% grid showing a significant increase. The WH, NE, and coastal regions show the highest increase whereas, the IP and NC regions show the lowest increase under the three GWLs. Further, we have calculated the change in

Table 2 Models performance of mean temperature (TMm) and Heatwave indices

Models	Mean	SPAEF	PBIAS (%)	Mean	SPAEF	PBIAS (%)
	<i>Mean temperature</i>			<i>HWN</i>		
Observed	25.2			15.96		
ACCESS-CM2	25.19	0.33	−0.03	17.63	−0.1	10.47
ACCESS-ESM1-5	25.19	0.32	−0.03	15.93	−0.13	−0.15
BCC-CSM2-MR	25.19	0.35	−0.05	19.05	−0.02	19.41
CanESM5	25.19	0.33	−0.05	16.85	−0.04	5.62
EC-Earth3	25.19	0.36	−0.03	19.19	−0.11	20.28
EC-Earth3-Veg	25.19	0.35	−0.03	19.98	0.1	25.2
INM-CM4-8	25.19	0.34	−0.05	17.43	−0.09	9.26
INM-CM5-0	25.19	0.34	−0.05	16.65	−0.12	4.36
MPI-ESM1-2-HR	25.19	0.36	−0.03	23.24	−0.04	45.63
MPI-ESM1-2-LR	25.19	0.34	−0.04	23.4	−0.22	46.65
MRI-ESM2-0	25.19	0.34	−0.03	23.63	0.04	48.06
NorESM2-LM	25.19	0.33	−0.05	20.77	−0.16	30.13
<i>NorESM2-MM</i>	<i>31.29</i>	<i>0.26</i>	<i>24.15</i>			
Ensemble	25.19	0.31	−0.04	19.48	−0.12	22.08
	<i>HWAS</i>			<i>HWD</i>		
Observed	8.54			10.47		
ACCESS-CM2	9.82	−0.1	14.95	11.33	−0.04	8.19
ACCESS-ESM1-5	11.42	−0.13	33.72	11.31	−0.09	8.02
BCC-CSM2-MR	9.15	−0.1	7.11	11.36	0.01	8.49
CanESM5	11.43	−0.13	33.83	11.73	−0.1	11.98
EC-Earth3	10.87	−0.11	27.35	12.52	−0.11	19.55
EC-Earth3-Veg	11.92	0.12	39.56	13.72	0.13	30.96
INM-CM4-8	12.43	0.001	45.62	12.8	0.01	22.21
INM-CM5-0	11.56	−0.28	35.43	11.84	−0.21	13.02
MPI-ESM1-2-HR	13.01	−0.08	52.39	16.04	0.003	53.14
MPI-ESM1-2-LR	13.53	−0.14	58.49	16.59	−0.16	58.43
MRI-ESM2-0	12.95	−0.06	51.7	16.27	−0.04	55.39
NorESM2-LM	12.28	−0.08	43.83	14.55	−0.11	38.94
Ensemble	11.7	−0.17	37	13.34	−0.12	27.36
	<i>HWAI</i>			<i>HWMI</i>		
Observed	33.02			32.65		
ACCESS-CM2	33.35	−0.11	1	29.48	−0.13	−9.7
ACCESS-ESM1-5	33.25	−0.21	0.7	27.94	−0.29	−14.4
BCC-CSM2-MR	33.49	−0.53	1.43	30.89	−0.27	−5.39
MRI-ESM2-0	33.18	−0.22	0.48	26.15	−0.44	−19.9
EC-Earth3	33.45	−0.5	1.31	29.24	−0.23	−10.44
EC-Earth3-Veg	33.47	0.01	1.36	29.56	0.04	−9.44
INM-CM4-8	33.46	−0.19	1.32	27.89	−0.1	−14.55
INM-CM5-0	33.35	−0.27	1.01	27.36	−0.25	−16.2
MPI-ESM1-2-HR	33.5	−0.45	1.47	31.11	−0.23	−4.71
MPI-ESM1-2-LR	33.47	−0.42	1.37	30.99	−0.29	−5.07
MRI-ESM2-0	33.52	−0.24	1.5	31.5	−0.31	−3.5
NorESM2-LM	33.44	−0.14	1.27	30.66	−0.23	−6.08
Ensemble	33.41	−0.43	1.18	29.4	−0.25	−9.95

heatwave indices for 2021–2050 (T1) and 2071–2100 (T2) periods. For all India, the HWN would increase by 2.5, and 4.2 times (19.64, and 44 events) under T1 and T2 periods

from the base period with more than 80% significant grids. Mishra et al., (2017) predict an increase of 3–9 and 16–30 severe heat wave events from 1971 to 2000 over India for the

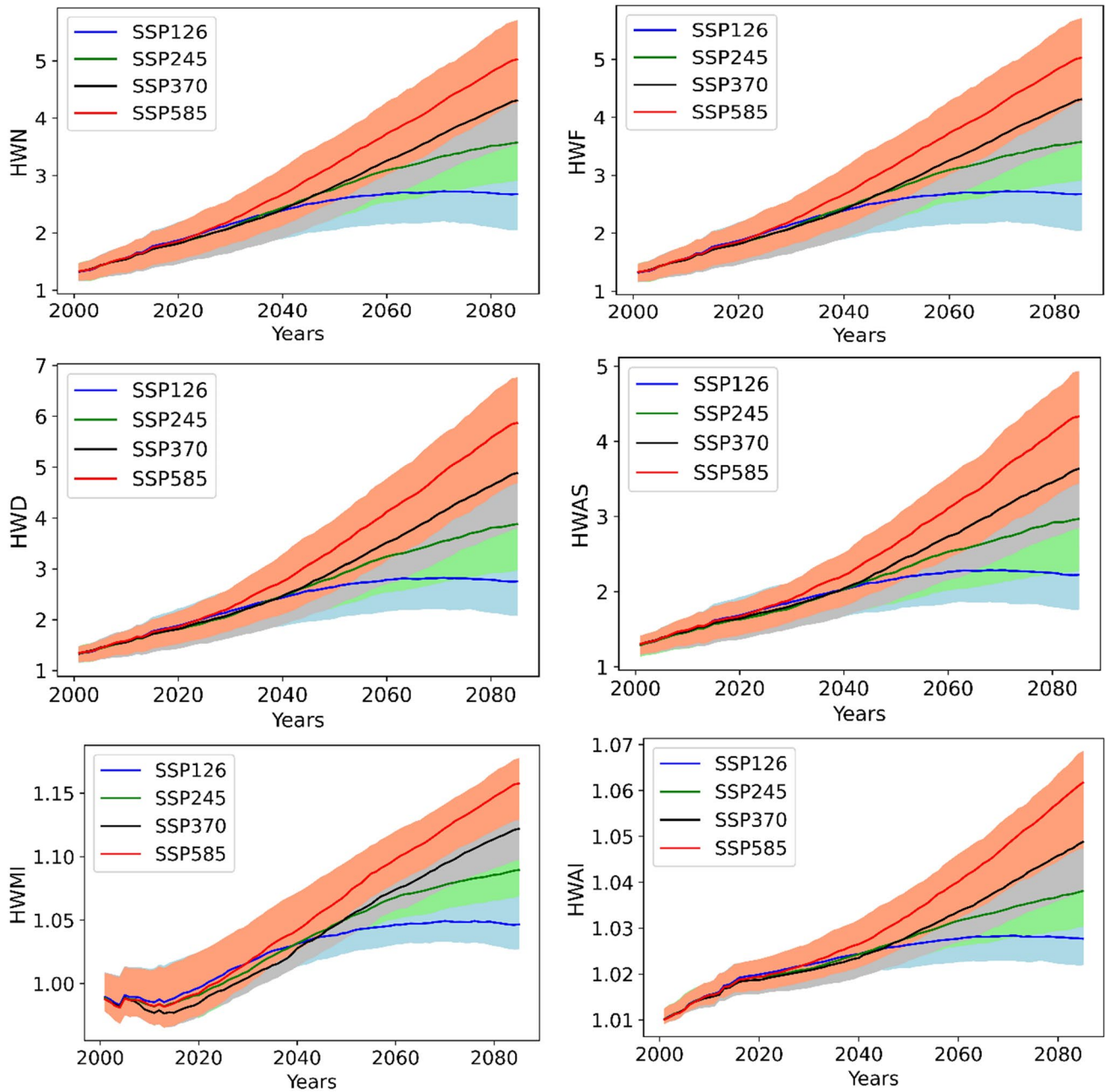


Fig. 2 Ratio of all India averaged heatwave indices analysed based on the Excess Heat Factor (EHF) during the period 2001–2086 with respect to the base period. Solid lines show the ensemble average, and

the shaded areas indicate the 25th and 75th percentiles of the model ensemble, representing the projection uncertainty

periods of 2021–2050 and 2071–2100, respectively, under the RCP8.5 scenario.

The all India mean HWF increase by 2.19, 2.78, and fourfold (9.7%, 15.7%, and 27%) from the base period with more than 71%, 88%, and 96% of the grid showing a significant increase under 1.5, 2, and 3 °C GWL, respectively. The NE region shows the highest increase under 1.5 °C and 2 °C GWL. Whereas under 3 °C GWL, WC shows

the highest increase. IP and NC show the lowest increase under 1.5, 2, and 3 °C GWL, respectively.

For all India, the HWF increased by 2.5 and 4.2 times (12.84% and 28.74%) from the baseline period with 82% and 98.45% grids showing significant increases under T1 and T2 periods, respectively. Mukherjee and Mishra (2018) found that the number of 3-consecutive hot days and nights increased 4–5 times at the middle of the century and 12

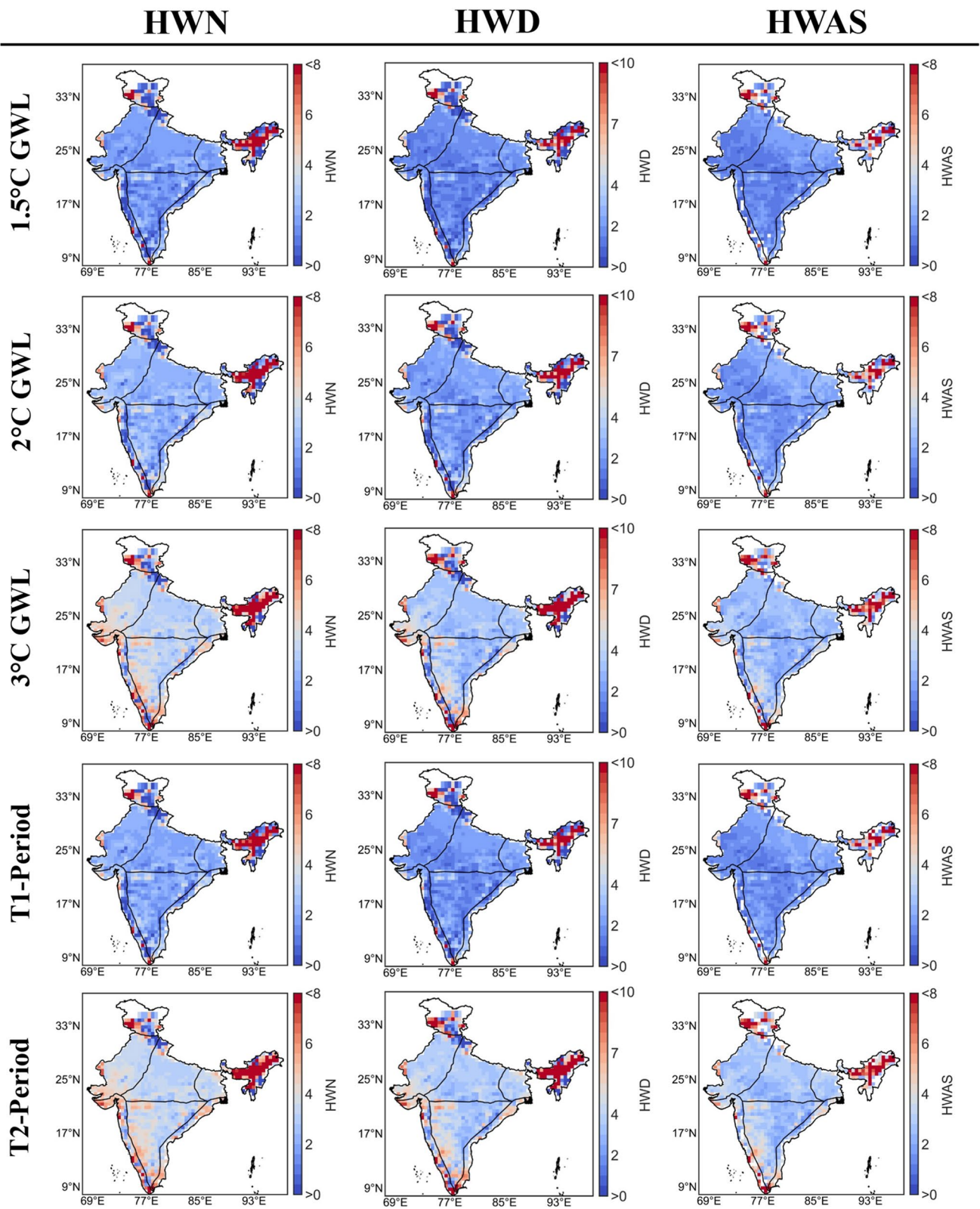


Fig. 3 Spatial distribution of the ratio with respect to the base period of heatwave indices calculated based on the Excess Heat Factor (HWN, HWD, HWAS) under 1.5 °C, 2 °C, 3 °C GWL and two time periods T1 (2021–2050) and T2 (2071–2100)

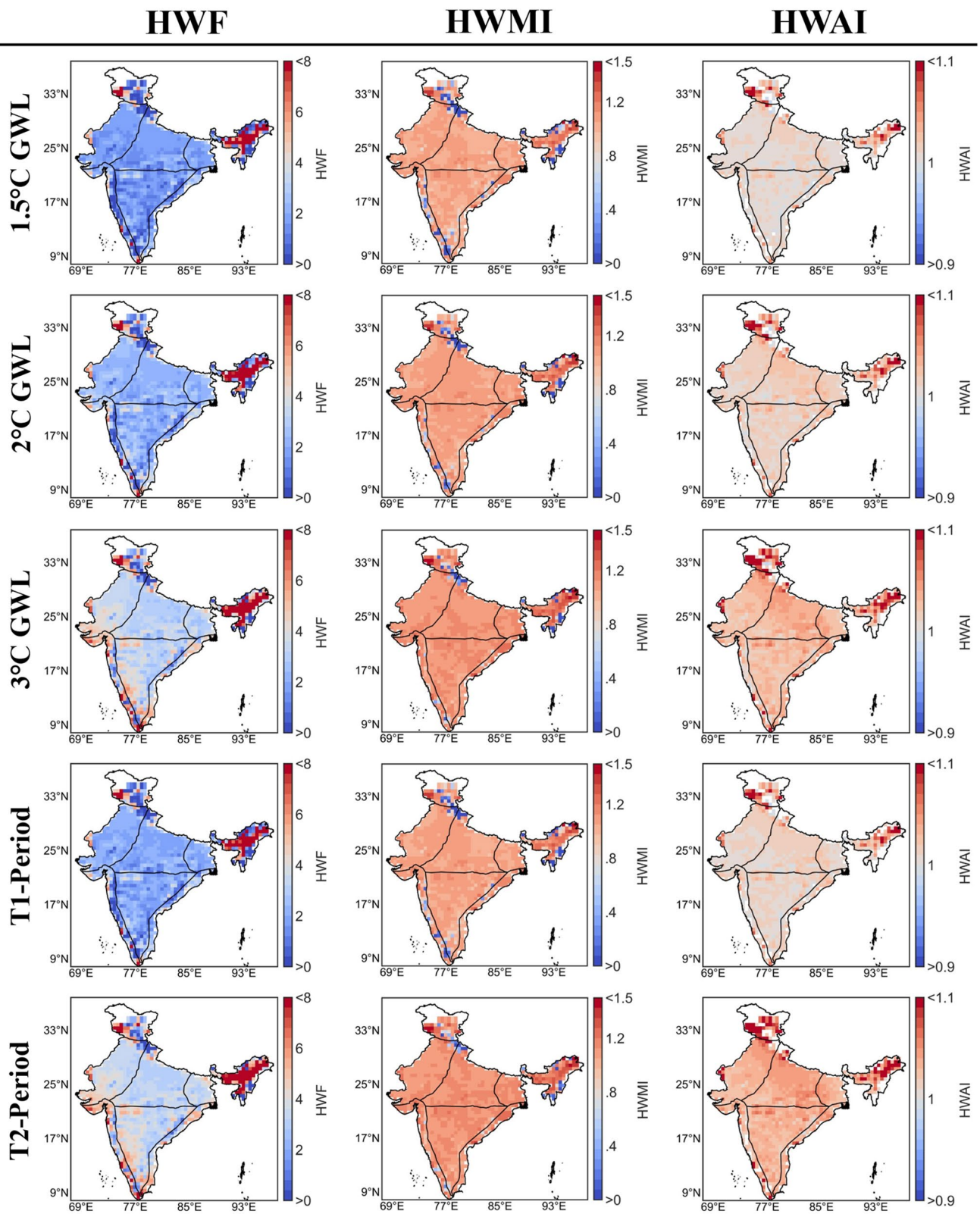


Fig. 4 Spatial distribution of the ratio with respect to the base period of heatwave indices calculated based on the Excess Heat Factor (HWF, HWMI, HWAI) under 1.5 °C, 2 °C, 3 °C GWL and two time periods T1 (2021–2050) and T2 (2071–2100)

times increase at the end of the century under RCP8.5 in India. For all India, the HWD increased 2.25, 2.9, and 4.35-fold (10, 16.6, and 30.7 days) from the base period with 58.35%, 83%, and 96% of grids showing a significant change under 1.5, 2, and 3 °C GWL, respectively. The NE region shows the highest change followed by WH and WC regions under 1.5, 2, and 3 °C GWL, respectively while IP and NC regions show the lowest increase under the three GWL. For all India, the HWD increased by 2.6, and 4.7 times (13.5, and 34.13 days) from the baseline period with 73.7% and 96.23% grids showing significant increases under T1 and T2 periods, respectively. Overall, the analysis found that the frequency and duration of heatwaves are projected to increase significantly across India under all three warming scenarios.

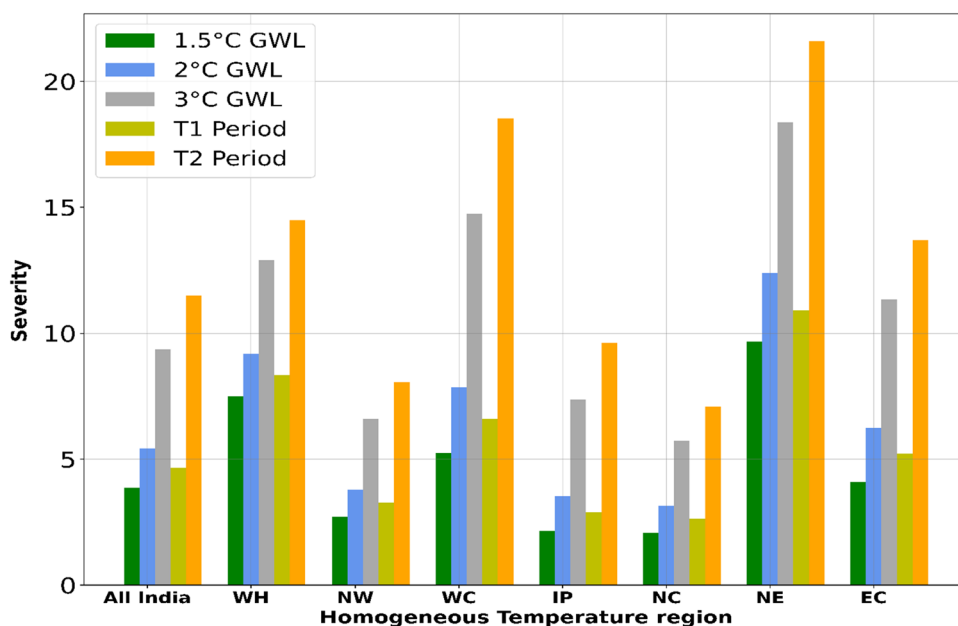
HWAS increased by 1.8, 2.22, and threefold (5.86, 9.3, and 16.74 days) from the base period with 30.24%, 57%, and 90% of grids showing a significant change under 1.5, 2, and 3 °C GWL, respectively (Fig. S5). The WH region shows the highest change followed by NE and WC regions under 1.5, 2, and 3 °C GWL, respectively. IP and NC regions show the lowest increase under 1.5, 2, and 3 °C GWL, respectively. For all India, the HWAS increased by 2, and 3.4 times (7.7, and 19.39 days) from the baseline period with 46.4% and 87.3% grids showing significant increases under T1 and T2 periods, respectively. HWAI and HWMI show the highest increment in the WH region followed by NE and WC under 1.5, 2, and 3 °C GWL. The temporal distribution ratio of HWSL for all SSP is depicted in Fig. S6. Additionally, Fig. S6 illustrates the change in number of days for the summer length of the heatwave (HWSL) in different warming periods. The study found that the duration of the heatwave (HWSL) increased by 1.7, 2, and 2.6 times

(16.46, 25.23, and 36.67 days) than the base period under 1.5, 2, and 3 °C global warming levels, respectively. The WC region showed the highest increase, followed by EC, and NE. The IP and NC regions had the lowest increase under 1.5, 2, and 3 °C global warming levels, respectively. Overall, India experienced an increase in HWSL by 2 and 3 times (21 and 46 days) more from the base period in the T1 and T2 periods, respectively. The results show that the length of the summer heatwave (HWSL) increases continuously due to the early onset of the heatwave (Rao et al. 2023). Figures S7–S10 show the spatial distribution of the ratio of multi-models mean of heatwave indices under 1.5 °C, 2 °C, 3 °C GWL, and two time periods (T1 and T2) concerning the base period for SSP1-2.6, SSP2-4.5, SSP3-7.0, and SSP5-8.5, respectively.

4.3 Changes in heatwave severity

We calculate the average heat wave severity of summer months (March–July) for all homogeneous temperature regions of India based on EHF under different warming scenarios. Fig. S11 shows the change in spatial distribution of severity under the three GWL and T1 and T2 periods. The severity of heat waves increased significantly in all regions under all warming scenarios (Fig. S12). The severity increases by 3.85, 5.4, and 9.4-folds under 1.5 °C, 2 °C, and 3 °C GWL, respectively (with respect to base period). The NE (9.68, 12.4, and 18.4-times) is the most vulnerable region followed by WH (7.5, 9.2, and 12.9-times), WC (5.3, 7.8, and 14.7-times) and EC (4.1, 6.2, and 11.3-times) under all warming scenarios. The IP (2.2, 3.5, and 7.4 times) and

Fig. 5 Regional mean of the multi-model ensemble of the ratio of heatwave severity calculated based on the Excess Heat Factor with respect to the base period under different warming levels



NC (2.1, 3.15, and 5.72 times) show the least increase in the severity under the three warming scenarios (Fig. 5).

We also calculated the average monthly severity ratio of future and current periods for all India. For a 30-year running window centred on each year from 2006 to 2085, the ratio of the severity to the current world (1991–2020, 30-year window centred on 2005) was calculated. The results showed that heat wave severity is projected to increase significantly in all summer months, especially in March and April months. By the end of the century, the March and April month heat wave severity increased 18 and 9 times than the current levels, respectively. From 2044, the severity in March months is expected to increase exponentially and reaching 6 times higher than the current period by the end of the century. The analysis of heat wave severity during the months of May, June, and July indicates a consistent upward trend, which is projected to persist until the end of the century, it will reach 4.75, 4.34, and 5.24 folds higher than the current period, respectively (Fig. 6).

4.4 Projected population exposure to HW under different warming levels

We analysed the total exposure, population effect, climate effect, and their interaction effect under three different warming levels (1.5, 2, and 3 °C) and two time periods for each of the four SSPs. The analysis covered 19 combinations of SSP, warming level, and time periods, as SSP1-2.6 did not achieve the 3 °C warming level. Population exposure is expected to increase in all SSPs and under warming, with SSP3 showing the most rapid increase due to its high population growth scenario. It is also observed that the population growth first increases and then decreases (Chen and

Sun 2019) over India in all the SSPs except in SSP3. Fig. S13 shows the changes in population exposure over time. As the global warming level increases from 1.5 to 3 °C, the total population exposure also increases across all SSPs (Fig. 7). The exposure patterns in SSP3-7.0 and SSP2-4.5 scenarios are similar across all homogeneous regions and warming levels. The WC region has the highest exposure, followed by the NE and EC regions in all SSPs and warming levels, while the WH region has the smallest exposure. To determine the relative importance of climate change and population growth, we calculated the climate and population effects. It was found that climate change has a greater influence than population growth for all SSPs and regions in India (Fig. 8).

For SSP3-7.0, under 1.5, and 2 °C GWL, the contribution of climate (48%, and 42%) and interaction effect (26%, and 34%) to the total exposure is higher than the population effect (25% and 24%). However, under a 3 °C GWL, the interaction effect's contribution across India is higher (43%) than the climate's (38%) and the population's (19%) effects. Climate effect (45%) makes a greater contribution than interaction effect (31%) and population effect (24%) in time period T1. By the end of the century the interaction effect (48%) will have a greater contribution than the population effect (16%) and climate effect (36%) (Fig. 8). Under all warming scenarios, the climate effect shows a greater contribution to total exposure under SSP1-2.6, SSP2-4.5, and SSP5-8.5 respectively. While interaction effect and population effect show moderate contribution in all SSPs. The findings indicate a decline in the population effect and a rise in the climate effect as global warming increases across all SSPs in the homogeneous regions, with the exception of the WH region. When the GWLs increased from 1.5 to 2 °C

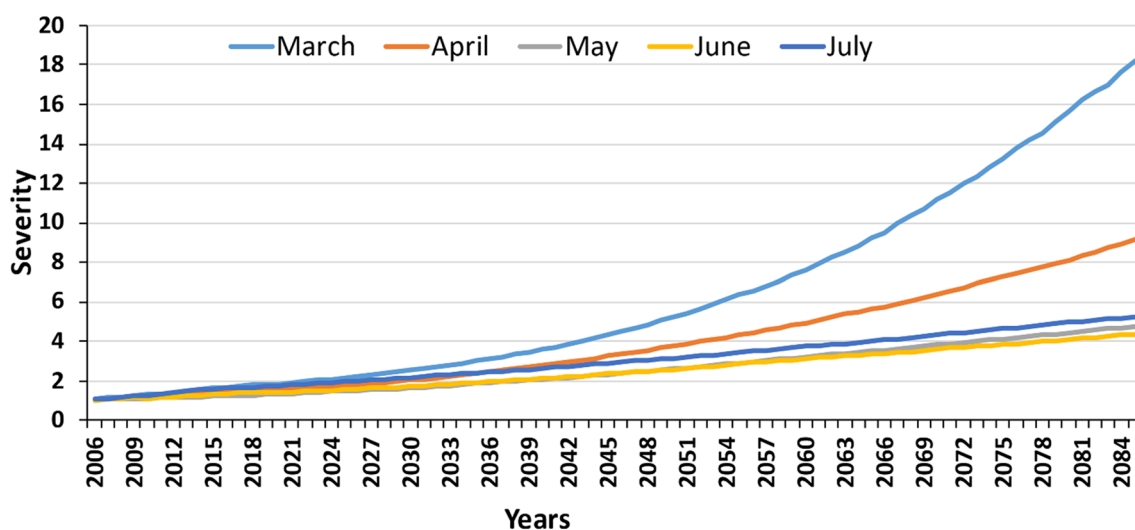


Fig. 6 Monthly mean of the multi-model ensemble of the ratio of heatwave severity calculated based on the Excess Heat Factor with respect to the current period (1991–2020) with the middle year 2005

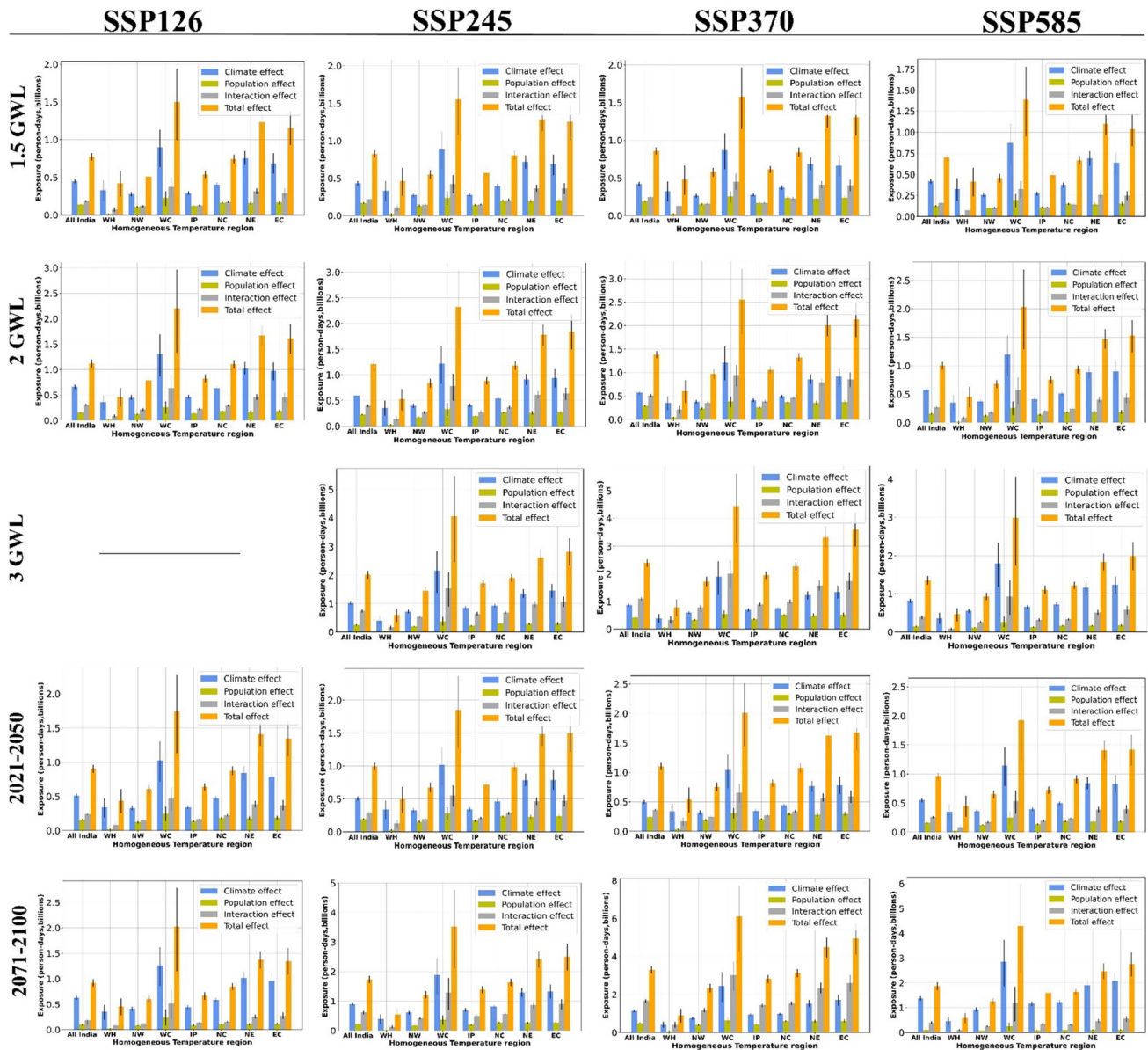


Fig. 7 Change in the climate, population, interaction, and total effect with respect to the base period under different SSPs in the 1.5, 2, 3 °C GWL, and two time periods 2021–2050 and 2071–2100. The column

shows the regional mean value and the bar depict the 90 and 10 percentile values obtained from the 100,000 bootstraps

under SSP1-2.6, SSP2-4.5, and SSP5-8.5, the overall exposure would increase by 1.4-fold, whereas, under SSP3-7.0, it would increase by 1.6-fold. Similarly, when the warming is increased from 2 to 3 °C, the total exposure would increase by 1.67 and 1.4 times under SSP2-4.5 and SSP5-8.5, respectively, whereas, it would increase by 1.73-fold in SSP3-7.0. From T1 to T2 period, the total exposure would increase by 1.03, 1.78, 3, and 2 times under SSP1-2.6, SSP2-4.5, SSP3-7.0, and SSP5-8.5 respectively, over India. In the IP region, the exposure increases at a greater rate compared to other homogeneous under all the SSPs.

Under SSP1-2.6, SSP2-4.5, SSP3-7.0, and SSP5-8.5, respectively, the total exposure for all India is expected to increase by 46%, 48%, 60%, and 44% by limit at 1.5 °C rather than 2 °C. All India's total exposure would decrease by 67%, 73%, and 37% under SSP2-4.5, SSP3-7.0, and SSP5-8.5 if the GWL was restricted to 2 °C (rather than 3 °C). The highest benefit observed in SSP3-7.0 is due to the high population growth rate (Maurya et al. 2023). The IP and WH regions would have the greatest and smallest benefit in total exposure, respectively, if we restricted the GWL to 1.5 °C and 2 °C. Since the population is expected to grow quickly in SSP3

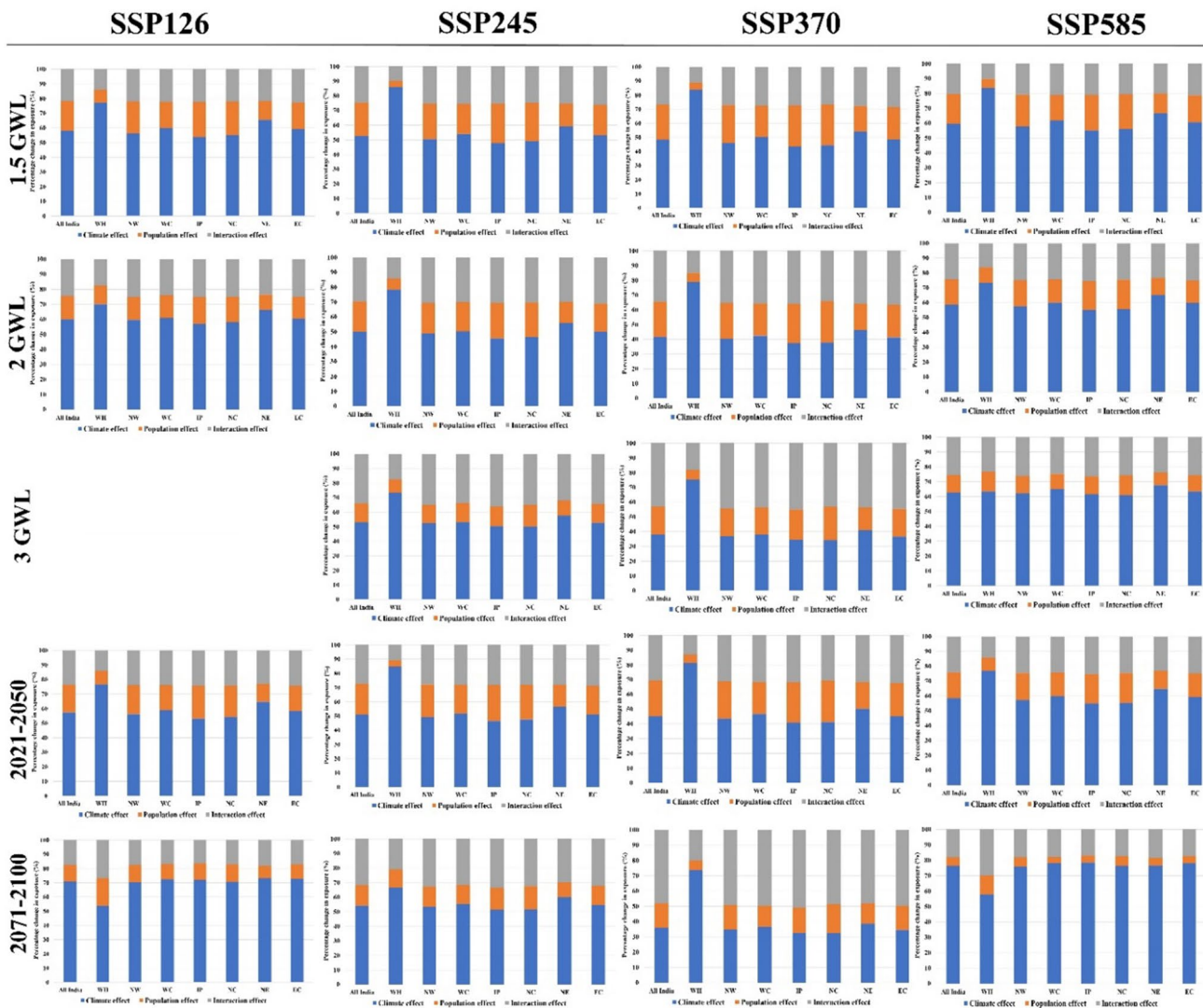


Fig. 8 Contribution of the change in population, climate, and their interaction on the exposure of the different scenarios in the 1.5, 2, 3 °C GWL, and two time periods. Unit is %

scenarios, SSP3-7.0 rather than SSP5-8.5 shows a rapid rise in overall exposure. Chen and Sun (2019) noted a similar finding for precipitation extremes. According to Das et al., (2022), heatwaves and droughts emerge as the most significant compound events influencing population exposure, magnifying the impact by a factor ranging from 2.52 to 4.69 in comparison to the historical period under SSP3-7.0. According to the current study, the change in total exposure of approximately 1.5 billion person-day under SSP5-8.5 and 2.5 billion person-day for SSP3-7.0 under 3 °C GWL. The present study reports climate, population, and interaction effects of approximately 0.93, 0.44,

and 1.16 billion person-day respectively for SSP3-7.0 under 3 °C GWL (Fig. 7).

5 Discussion

The present study deals with the future change in heatwave characteristics and severity with associated population exposure in homogenous temperature regions of India using CMIP6 under different GWLs over two time periods. Most of the CMIP6 models showed good spatial agreement

with the observed data. The current study employed the period from March to August to identify possible shifts in the occurrence of heat wave events in regions characterized by elevated temperatures. The results clearly depict a significant increase in heatwave events, and the severity becomes more pronounced as warming increases in the different homogeneous regions of India. Heatwaves are caused by rising atmospheric pressure because the falling air is compressed and heated (Jakob and Reeder 2021, IPCC 2013). The Himalayan, Coastal, and Northeastern regions of India showed a pronounced increase in heatwave characteristics and heatwave severity under all warming levels. Das and Umamahesh (2022) also report that the Himalayan, eastern coast, and southern part of India were affected by heatwaves from 2020–2046 to 2074–2100. The IP and NC regions showed the lowest increase. Numerous physical factors contribute to these changes, such as the urban heat island effect, solar variability, climate change, shifts in cloud cover, modified atmospheric circulation, warming oceans, local influences, human activities, and the impact of heatwaves (Meehl and Tebaldi 2004; Roemmich et al. 2007; Santamouris 2014; Mukherjee and Mishra 2018). Most parts of the IP and NC were irrigated regions. Irrigation affects the surface energy budget across the area by increasing the latent heat flux and reducing the sensible heat flux (Mukherjee and Mishra 2018). The reduced surface air temperature is the result of an increase in the latent heat flux and relative humidity, which also improves evaporative cooling. Therefore, increased evaporative cooling results in a rapid increase in heat waves (Mueller et al. 2016; Mukherjee and Mishra 2018; Srivastava et al. 2022). The coastal regions of India are at high risk of heat wave severity due to El Niño-Southern Oscillation (ENSO) events and their tropical monsoon climate, with high temperatures and humidity throughout the year (Dash et al. 2007; Mukherjee and Mishra 2018; Joseph et al. 2019). The WH region experiences extreme heat during summer due to its geographical location (tropical and subtropical zones), the effects of global warming, and the heat island effect caused by urbanization (Dimri and Dash 2012; Rana et al. 2020; Singh et al. 2021). The heat wave severity for May, June, and July showed a linear increase by the end of the century. The results showed an exponential increase in severity during March and April by the end of the century. This change indicates the early onset of summer due to rapid climate change. This rapid change has a significant impacts on agriculture, economic losses, human health, work force, energy demand, ecosystems over India (IPCC 2014; Mazdiyasn et al. 2017; Perkins-Kirkpatrick and Lewis 2020; Nishant et al. 2022).

Furthermore, we examined the variation in population susceptibility to heatwave events under different global warming levels (GWL). A significant increase in exposure

to heat waves was found under SSP3-7.0, followed by SSP5-8.5, SSP2-4.5, and SSP1-2.6, because of the high growth rate in the population under SSP3-7.0 (Chen and Sun 2019; Ma and Yuan 2021). The contribution of climate to the total exposure is more pronounced than that of the population and the interaction effect under all SSPs, except SSP3-7.0. The current result is consistent with those of Das et al. (2022) and Liu et al. (2017), who reported that for India, the climate and interaction impacts dominate the population effect. Furthermore, Liu et al. (2017) reported that in India, the interaction effect contributes more to the high emission scenario (SSP3-7.0) towards the end of the century. The findings indicate that the coastal and northeastern regions exhibited the highest levels of exposure. The IP region would experience the greatest benefits among all homogeneous regions in terms of limiting global warming, primarily because of its high population density. In contrast, the WH region showed the lowest exposure due to the lower population density.

The analysis did not consider the effects of adaptive measures, migration, and urbanization on population exposure. It relies on decadal population data and uses linear interpolation to estimate yearly figures, potentially introducing uncertainties. Additionally, the reliability of the projections was influenced by uncertainties in the CMIP6 models and population projections. We address the need to understand how heatwaves evolve at different warming levels, providing timely insights that can contribute to the development of climate adaptation and mitigation policies in the near to intermediate future. Our research encompasses both the characteristics of heatwaves and an evaluation of the corresponding population exposure under distinct degrees of warming. The outcomes of this research will provide valuable insights to decision-makers, enabling them to enhance their strategies for both mitigating and adapting to climate change. Additionally, these findings will aid in effective climate risk management for the future.

6 Summary and conclusion

In this study, we focus on analysing characteristics of heatwaves and associated population exposure in India under the present and future warming scenarios. First, we estimated the performance of historical mean temperature of climate models to enhance comprehension of future climate scenarios. Based on the performance of the models, we selected the 12 best-performing models for further ensemble analysis. Further, we estimated the climatology and changes in summer heat wave severity and associated heatwave events based on EHF and population exposure over India under 1.5, 2 and 3 °C global warming scenarios along with two time periods using CMIP6. The results show the early onset of heatwaves in coming years that could significantly affect the

population and agriculture. The irrigated areas (IP and NC) of India showed less increase in heatwave characteristics due to the cooling effect of evaporation whereas humid coastal areas (EC and WC) showed comparatively higher increases as warming increases. Some of the key findings of the study are highlighted as follows:

- India is anticipated to face exaggerated frequency, duration, peak, and mean intensity of heat waves with increasing GWL.
- The severity of heatwaves in March and April is escalating more rapidly compared to the months of May, June, and July, as compared to the current world (1990–2020).
- The WH region exhibits the most pronounced increase in heatwave severity, followed by the WC, NE, and EC regions after 2050 from the base period.
- Pronounced increases are projected in heatwave frequency (HWN (44 events) and HWF (29%)), duration (HWD (34 days) and HWAS (19 days)) and intensity (HWTI (3.35 °C) and HWAI (1.3 °C)) by the end of the century compared to the base period.
- Coastal, Northeastern, and Himalayan regions exhibit the most substantial changes from the baseline.
- The projection of total exposure and their contributing factors are expected to increase in all SSPs under different warming.
- There will be significant regional variations in population exposure, with the WC, NE, and EC regions becoming high-population exposure areas and the WH region becoming the least exposed.

Supplementary Information The online version contains supplementary material available at <https://doi.org/10.1007/s00477-024-02695-2>.

Author contribution All authors contributed to the study conception and design. HKM: data curation, investigation, conceptualization, writing. NJ: conceptualization, methodology and editing. SS: methodology and editing.

Funding The authors declare that no funds, grants, or other support were received during the preparation of this manuscript.

Data availability The Bias corrected CMIP6 data sets used in the study are available at <https://zenodo.org/record/3873998#.Y7xgynZBy01> for the Indian region at 0.25°*0.25 grid given by Mishra et al. 2020 and the population data are available at 1/8° resolution for the four Shared Socioeconomic Pathways (SSPs). The Population datasets were downloaded from the Socioeconomic Data and Applications Centre (SEDAC) <https://sedac.ciesin.columbia.edu/data/set/popdynamics-1-km-downs-caled-pop-base-year-projection-ssp-2000-2100-rev01/data-download>.

Availability of data and materials Some or all data, models that support the findings of this study are available from the corresponding author upon reasonable request.

Code availability Available on request.

Declarations

Competing interests The authors declare no competing interests.

Conflict of interests The authors have no relevant financial or non-financial interests to disclose.

Consent for publication All the authors approved the manuscript for publication. This work is not published elsewhere.

Ethics approval Not applicable.

References

- Andrews O, Le Quéré C, Kjellstrom T et al (2018) Implications for workability and survivability in populations exposed to extreme heat under climate change: a modelling study. *Lancet Planet Health* 2:e540–e547
- Chen H, Sun J (2019) Increased population exposure to extreme droughts in China due to 0.5°C of additional warming. *Environ Res Lett* 14:064011
- Chen H, Sun J (2021) Significant increase of the global population exposure to increased precipitation extremes in the future. *Earth's Fut* 9:e2020EF001941. <https://doi.org/10.1029/2020EF001941>
- Chen H, Sun J, Li H (2020) Increased population exposure to precipitation extremes under future warmer climates. *Environ Res Lett* 15:034048
- COP26 Goals—UN Climate Change Conference (COP26) at the SEC—Glasgow 2021. <https://webarchive.nationalarchives.gov.uk/ukgwa/20230311034236/https://ukcop26.org/cop26-goals/>. Accessed 9 Nov 2023
- Dahl K, Licker R, Abatzoglou JT, Delet-Barreto J (2019) Increased frequency of and population exposure to extreme heat index days in the United States during the 21st century. *Environ Res Commun* 1:075002
- Das J, Umamahesh NV (2022) Heat wave magnitude over India under changing climate: projections from CMIP5 and CMIP6 experiments. *Int J Climatol* 42:331–351. <https://doi.org/10.1002/joc.7246>
- Das J, Manikanta V, Umamahesh NV (2022) Population exposure to compound extreme events in India under different emission and population scenarios. *Sci Total Environ* 806:150424
- Dash SK, Mamgain A (2011) Changes in the frequency of different categories of temperature extremes in India. *J Appl Meteorol Climatol* 50:1842–1858
- Dash SK, Jenamani RK, Kalsi SR, Panda SK (2007) Some evidence of climate change in twentieth-century India. *Clim Change* 85:299–321. <https://doi.org/10.1007/s10584-007-9305-9>
- Dimri AP, Dash SK (2012) Wintertime climatic trends in the western Himalayas. *Clim Change* 111:775–800
- Dwivedi YK, Hughes L, Kar AK et al (2022) Climate change and COP26: are digital technologies and information management part of the problem or the solution? An editorial reflection and call to action. *Int J Inf Manag* 63:102456. <https://doi.org/10.1016/j.ijinfomgt.2021.102456>
- Guleria S (2018) Heat wave in India, Documentation of State of Telangana and Odisha, 2016. National Institute of Disaster Management
- Harrington LJ, Otto FE (2018) Changing population dynamics and uneven temperature emergence combine to exacerbate regional exposure to heat extremes under 1.5°C and 2°C of warming. *Environ Res Lett* 13:034011

- IPCC (2013) Technical Summary — IPCC. <https://www.ipcc.ch/report/ar5/wg1/technical-summary/>. Accessed 14 Mar 2024
- IPCC (2014) Climate change 2014: synthesis report. Contribution of Working Groups I, II and III to the fifth assessment report of the Intergovernmental Panel on Climate Change. Ipcc
- IPCC (2021) Climate Change 2021 – The Physical Science Basis: Working Group I Contribution to the Sixth Assessment Report of the Intergovernmental Panel on Climate Change, 1st ed. Cambridge University Press. <https://doi.org/10.1017/9781009157896>
- Jakob C, Reeder M (2021) The Science of Heat Waves Explained | KQED. <https://www.kqed.org/news/11880497/the-science-of-heat-waves-explained>. Accessed 15 Mar 2024
- Jones B, O'Neill BC, McDaniel L et al (2015) Future population exposure to US heat extremes. *Nat Clim Change* 5:652–655. <https://doi.org/10.1038/nclimate2631>
- Joseph D, Liya VB, Rojith G et al (2019) Time series analysis of CMIP5 Model and observed sea surface temperature anomaly along Indian Coastal Zones. *J Coastal Res* 86:239–247
- Keggenhoff I, Elizbarashvili M, King L (2015) Heat wave events over Georgia since 1961: climatology, changes and severity. *Climate* 3:308–328
- Koch J, Demirel MC, Stisen S (2018) The SPAtial EFficiency metric (SPAEF): multiple-component evaluation of spatial patterns for optimization of hydrological models. *Geosci Model Dev* 11:1873–1886
- Kothawale DR, Rupa Kumar K (2005) On the recent changes in surface temperature trends over India. *Geophys Res Lett*. <https://doi.org/10.1029/2005GL023528>
- Li D, Zhou T, Zou L et al (2018) Extreme high-temperature events over East Asia in 1.5°C and 2°C warmer futures: analysis of NCAR CESM low-warming experiments. *Geophys Res Lett* 45:1541–1550
- Li D, Yuan J, Kopp RE (2020) Escalating global exposure to compound heat-humidity extremes with warming. *Environ Res Lett* 15:064003. <https://doi.org/10.1088/1748-9326/ab7d04>
- Liu Z, Anderson B, Yan K et al (2017) Global and regional changes in exposure to extreme heat and the relative contributions of climate and population change. *Sci Rep* 7:43909. <https://doi.org/10.1038/srep43909>
- Ma F, Yuan X (2021) Impact of climate and population changes on the increasing exposure to summertime compound hot extremes. *Sci Total Environ* 772:145004
- Maurya HK, Joshi N, Swami D, Suryavanshi S (2023) Change in temperature extremes over India under 1.5 °C and 2 °C global warming targets. *Theor Appl Climatol* 152:57–73. <https://doi.org/10.1007/s00704-023-04367-7>
- Mazdiyasi O, AghaKouchak A, Davis SJ et al (2017) Increasing probability of mortality during Indian heat waves. *Sci Adv* 3:e1700066
- McMichael AJ, Wilkinson P, Kovats RS et al (2008) International study of temperature, heat and urban mortality: the 'ISOTHURM' project. *Int J Epidemiol* 37:1121–1131
- Meehl GA, Tebaldi C (2004) More intense, more frequent, and longer lasting heat waves in the 21st century. *Science* 305:994–997. <https://doi.org/10.1126/science.1098704>
- Mishra V, Mukherjee S, Kumar R, Stone DA (2017) Heat wave exposure in India in current, 1.5°C, and 2.0°C worlds. *Environ Res Lett* 12:124012
- Mishra V, Bhatia U, Tiwari AD (2020) Bias-corrected climate projections for South Asia from coupled model intercomparison project-6. *Sci Data* 7:1–13
- Mueller ND, Butler EE, McKinnon KA et al (2016) Cooling of US Midwest summer temperature extremes from cropland intensification. *Nat Clim Chang* 6:317–322
- Mukherjee S, Mishra V (2018) A sixfold rise in concurrent day and night-time heatwaves in India under 2°C warming. *Sci Rep* 8:1–9
- Nageswararao MM, Sinha P, Mohanty UC, Mishra S (2020) Occurrence of more heat waves over the central east coast of India in the recent warming era. *Pure Appl Geophys* 177:1143–1155. <https://doi.org/10.1007/s00024-019-02304-2>
- Nairn J, Fawcett R (2011) Defining heatwaves: heatwave defined as a heat-impact event servicing all. *Europe* 220:224
- Nairn JR, Fawcett RJB (2014) The excess heat factor: a metric for heatwave intensity and its use in classifying heatwave severity. *Int J Environ Res Public Health* 12:227–253. <https://doi.org/10.3390/ijerph120100227>
- Nairn J, Ostendorf B, Bi P (2018) Performance of excess heat factor severity as a global heatwave health impact index. *Int J Environ Res Public Health* 15:2494. <https://doi.org/10.3390/ijerph15112494>
- Nishant N, Ji F, Guo Y et al (2022) Future population exposure to Australian heatwaves. *Environ Res Lett* 17:064030
- Nori-Sarma A, Benmarhnia T, Rajiva A et al (2019) Advancing our understanding of heat wave criteria and associated health impacts to improve heat wave alerts in developing country settings. *Int J Environ Res Public Health* 16:2089
- Oleson KW, Anderson GB, Jones B et al (2018) Avoided climate impacts of urban and rural heat and cold waves over the US using large climate model ensembles for RCP8.5 and RCP4.5. *Clim Change* 146:377–392
- Pai DS, Nair S, Ramanathan AN (2013) Long term climatology and trends of heat waves over India during the recent 50 years (1961–2010). *Mausam* 64:585–604
- Pattanaik DR, Mohapatra M, Srivastava AK, Kumar A (2017) Heat wave over India during summer 2015: an assessment of real time extended range forecast. *Meteorol Atmos Phys* 129:375–393
- Perkins SE, Alexander LV (2013) On the measurement of heat waves. *J Clim* 26:4500–4517. <https://doi.org/10.1175/JCLI-D-12-00383.1>
- Perkins-Kirkpatrick SE, Lewis SC (2020) Increasing trends in regional heatwaves. *Nat Commun* 11:3357
- Petrovic D, Fersch B, Kunstmann H (2023) Heat wave characteristics: evaluation of regional climate model performances for Germany. *Nat Hazards Earth Syst Sci Discuss* 2023:1–35
- Raei E, Nikoo MR, AghaKouchak A et al (2018) GHWR, a multi-method global heatwave and warm-spell record and toolbox. *Sci Data* 5:1–15
- Rana A, Nikulin G, Kjellström E et al (2020) Contrasting regional and global climate simulations over South Asia. *Clim Dyn* 54:2883–2901
- Rao KK, Reddy PJ, Chowdary JS (2023) Indian heatwaves in a future climate with varying hazard thresholds. *Environ Res Climate* 2:015002. <https://doi.org/10.1088/2752-5295/acb077>
- Ratnam JV, Behera SK, Ratna SB et al (2016) Anatomy of Indian heatwaves. *Sci Rep* 6:24395. <https://doi.org/10.1038/srep24395>
- Reddy JP, Perkins-Kirkpatrick SE, Sharples JJ (2021) Intensifying Australian heatwave trends and their sensitivity to observational data. *Earth's Future* 9(4):e2020EF001924. <https://doi.org/10.1029/2020EF001924>
- Roemmich D, Gilson J, Davis R et al (2007) Decadal spinup of the South Pacific subtropical gyre. *J Phys Oceanogr* 37:162–173
- Rohat G, Flacke J, Dosio A et al (2019) Projections of human exposure to dangerous heat in African cities under multiple socio-economic and climate scenarios. *Earth's Future* 7:528–546. <https://doi.org/10.1029/2018EF001020>
- Rohini P, Rajeevan M, Srivastava AK (2016) On the variability and increasing trends of heat waves over India. *Sci Rep* 6:1–9
- Rohini P, Rajeevan M, Mukhopadhyay P (2019) Future projections of heat waves over India from CMIP5 models. *Clim Dyn* 53:975–988

- Santamouris M (2014) Cooling the cities—a review of reflective and green roof mitigation technologies to fight heat island and improve comfort in urban environments. *Sol Energy* 103:682–703
- Schleussner C-F, Lissner TK, Fischer EM et al (2016) Differential climate impacts for policy-relevant limits to global warming: the case of 1.5 °C and 2 °C. *Earth Syst Dyn* 7:327–351. <https://doi.org/10.5194/esd-7-327-2016>
- Singh R, Kumar R (2019) Climate versus demographic controls on water availability across India at 1.5°C, 2.0°C and 3.0°C global warming levels. *Global Planet Change* 177:1–9. <https://doi.org/10.1016/j.gloplacha.2019.03.006>
- Singh S, Mall RK, Singh N (2021) Changing spatio-temporal trends of heat wave and severe heat wave events over India: an emerging health hazard. *Int J Climatol* 41:E1831–E1845
- Smirnov O, Zhang M, Xiao T et al (2016) The relative importance of climate change and population growth for exposure to future extreme droughts. *Clim Change* 138:41–53. <https://doi.org/10.1007/s10584-016-1716-z>
- Sonali P, Kumar DN (2013) Review of trend detection methods and their application to detect temperature changes in India. *J Hydrol* 476:212–227
- Srivastava A, Mohapatra M, Kumar N (2022) Hot weather hazard analysis over India. *Sci Rep* 12:19768
- Weber T, Bowyer P, Rechid D et al (2020) Analysis of compound climate extremes and exposed population in Africa under two different emission scenarios. *Earth's Fut* 8:e2019EF001473
- WMO WM (2020) State of the Global Climate 2020. <https://library.wmo.int/records/item/56247-state-of-the-globalclimate-2020#.YH2x9i2B2F2>
- Yu R, Zhai P, Lu Y (2018) Implications of differential effects between 1.5 and 2 °C global warming on temperature and precipitation extremes in China's urban agglomerations. *Int J Climatol* 38:2374–2385. <https://doi.org/10.1002/joc.5340>
- Zhang W, Zhou T, Zou L et al (2018) Reduced exposure to extreme precipitation from 0.5°C less warming in global land monsoon regions. *Nat Commun*. <https://doi.org/10.1038/s41467-018-05633-3>
- Zhou J, Teuling AJ, Seneviratne S, Hirsch A (2022) Increasing population exposure to future heatwaves influenced by land-atmosphere interactions. Preprint. <https://doi.org/10.21203/rs.3.rs-1990379/v1>

Publisher's Note Springer Nature remains neutral with regard to jurisdictional claims in published maps and institutional affiliations.

Springer Nature or its licensor (e.g. a society or other partner) holds exclusive rights to this article under a publishing agreement with the author(s) or other rightsholder(s); author self-archiving of the accepted manuscript version of this article is solely governed by the terms of such publishing agreement and applicable law.